Extreme Mechanics Letters 43 (2021) 101182

Contents lists available at ScienceDirect

Extreme Mechanics Letters

journal homepage: www.elsevier.com/locate/eml

Fatigue-resistant adhesion II: Swell tolerance

Wenlei Zhang [a], Jian Hu [a], Hang Yang [b], Zhigang Suo [b,*], Tongqing Lu [a,*]

[a] State Key Lab for Strength and Vibration of Mechanical Structures, Soft Machines Lab, International Center for Applied Mechanics, Department of Engineering Mechanics, Xi'an Jiaotong University, Xi'an 710049, China

[b] John A. Paulson School of Engineering and Applied Sciences, Kavli Institute for Bionano Science and Technology, Harvard University, MA 02138, United States

ARTICLE INFO

Article history:
Received 8 December 2020
Received in revised form 11 January 2021
Accepted 11 January 2021
Available online 18 January 2021

Keywords:
Swell tolerance
Fatigue resistant
Hydrogel adhesion
Microgel

ABSTRACT

In a previous paper (Zhang et al., 2020), we have demonstrated an adhesive of high fatigue threshold ~300 J/m^2 using an as-prepared hydrogel of long-chain polymer network. In most applications, however, hydrogel adhesives are in contact with water. The long-chain hydrogel swells and reduces the fatigue threshold. Here we demonstrate a type of swell-tolerant and fatigue-resistant hydrogel adhesive: a long-chain polymer network in topological entanglement with short-chain microgels. The short-chain microgels restrict swell, and the long-chain network retains the high fatigue threshold. After the hydrogel adhesives swell in water to equilibrium, the fatigue threshold is 61 J/m^2 for an adhesive of a long-chain network without microgels, and is 262 J/m^2 for an adhesive of a long-chain network with microgels.

1. Introduction

Adhesives are commonly made of polymers, including elastomers, thermoplastics, emulsions, thermosets, and biotissues [1]. In recent decades, hydrogel adhesives have been developed for tissue repair [2–5], drug delivery [6,7], bioelectronics [8–10], and implants [11,12]. In these applications, adhesion is commonly required to retain the wetness and elasticity of the adherends, the living tissues. Hydrogel adhesives readily achieve wet and elastic adhesion, but often have low toughness, on the order of 10 J/m^2 [13]. For example, protein hydrogels have low toughness [2,14] because they have low polymer contents and short chains [15]. In recent years, several hydrogel adhesives have achieved high toughness under monotonic load, on the order of 1000 J/m^2 [2,16]. These hydrogel adhesives achieve high toughness by incorporating sacrificial bonds. The sacrificial bonds, however, do not increase fatigue threshold under cyclic load. For example, an alginate–polyacrylamide hydrogel has high toughness [17] and high adhesion energy [2], but the adhesive grows a crack under cyclic load above a low threshold on the order of 10 J/m^2 [18].

Several recent papers have reported polymer networks of high fatigue thresholds [19–24]. Specifically, in a previous paper we have reported high fatigue threshold of ~300 J/m^2 using a hydrogel adhesive of a long-chain polymer network [25]. The high fatigue threshold was measured for an as-prepared hydrogel adhesive. In most applications, however, hydrogel adhesives are in contact with water. The long-chain hydrogels are prone to swell, and a fully swollen hydrogel adhesive is expected to have a low fatigue threshold. Here we demonstrate a type of swell-tolerant and fatigue-resistant hydrogel adhesives. Such an adhesive consists of a long-chain polymer network in topological entanglement with short-chain microgels. The short-chain microgels restrict swell, and the long-chain polymer network retains the high fatigue threshold. After the hydrogel adhesive swells in water to equilibrium, a fatigue threshold of 262 J/m^2 is achieved.

A long-chain hydrogel adheres two adherends either by bonds between the adhesive and adherends, or by topological entanglement of the polymer networks of the adhesive and adherends [26]. The hydrogel adhesive achieves high fatigue threshold by the Lake–Thomas mechanism [27]. Ahead of a crack tip, the covalent bonds of a polymer chain are stretched near the breaking point elastically before fracture (Fig. 1a). When a single covalent bond breaks, the elastic energy in the entire chain dissipates, leading to tough adhesion. The polymer chains are elastic dissipaters—they are elastic before breaking. This toughening mechanism operates under both monotonic load and cyclic load. In our previous demonstration with polyacrylamide hydrogel adhesives, when the average number of monomers per chain increases from 380 to around 38000, the fatigue threshold increases from 40 J/m^2 to 300 J/m^2, and the adhesion energy increases from 180 J/m^2 to 1400 J/m^2 [25].

Fatigue threshold of a hydrogel changes upon gaining or losing water [28]. Swell can be controlled by several methods, by

* Corresponding authors.
E-mail addresses: suo@seas.harvard.edu (Z. Suo), tongqinglu@mail.xjtu.edu.cn (T. Lu).

https://doi.org/10.1016/j.eml.2021.101182
2352-4316/

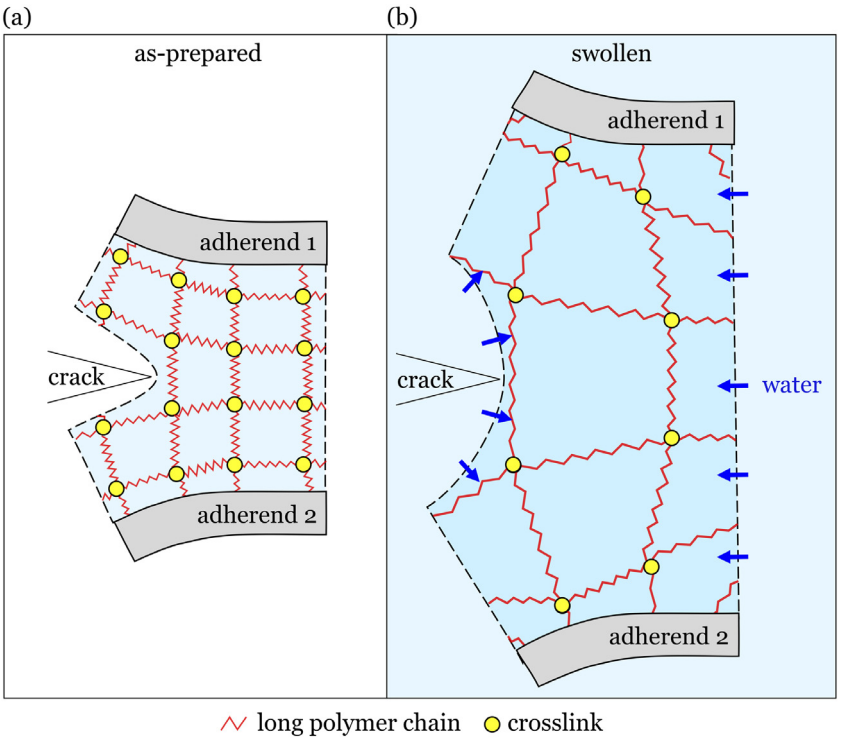

Fig. 1. Adherends bonded by a hydrogel adhesive. (a) In the as-prepared state, the hydrogel adhesive consists of a polymer network and a certain amount of water. (b) In contact with pure water, the hydrogel adhesive imbibes more water.

increasing crosslink density [29], activating noncovalent interactions [30,31], adding nanoparticles [32,33], copolymerizing hydrophilic and hydrophobic monomers [34,35], and casting a hydrogel in a non-swelling fabric [36]. Of particular relevance to this paper is the double network hydrogel of interpenetrating short-chain network and long-chain network [37]. When submerged in water to swell to equilibrium, the hydrogel-to-polymer mass ratio is 100 for a hydrogel of a single long-chain network, and is 6.25 for a double network hydrogel [19]. The short-chain network restricts swell, and the long-chain network gives high fatigue threshold [19,20]. None of these swell-tolerant hydrogels have been demonstrated as fatigue-resistant adhesives.

A double network hydrogel is synthesized by first forming the short-chain network, immersing it in the precursor of the long-chain network and then forming the long-chain network. The method is difficult to use to form adhesives. We have tried to first cure the short-chain hydrogel adhesive with adherends and then immerse the adhesive sample in the precursor. We find that due to the constrains of adherends, the brittle short-chain hydrogel adhesive swells and fractures into small pieces. By contrast, Hu et al. prepared the short-chain network in the form of microgels, and added them to the precursor of long-chain network [38]. We adopt this method to develop microgel-reinforced hydrogel adhesives (Fig. 2). The networks of microgels are topologically entangled with the long-chain network. The short-chain microgels have a much lower swelling ratio than the long-chain network hydrogel. Submerged in water, as long as the microgels do not rupture, the microgels can effectively restrict the overall swelling of microgel-reinforced hydrogels.

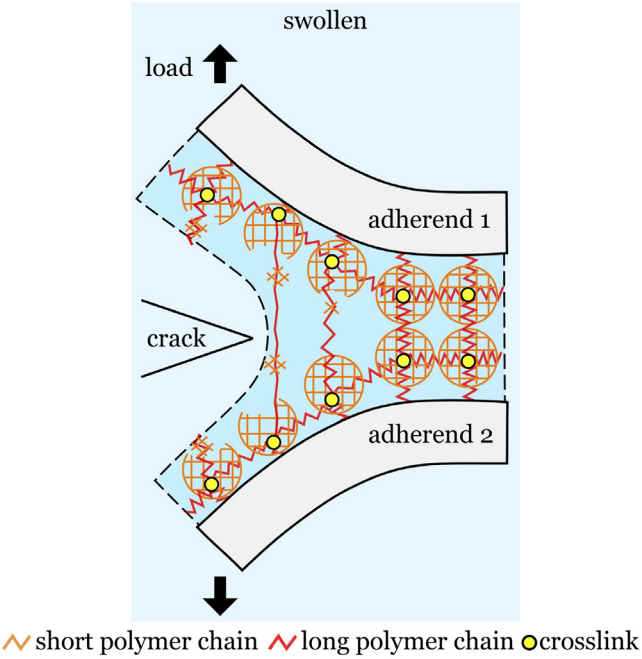

Fig. 2. Microgel-reinforced hydrogel adhesive. The long-chain polymer network of the adhesive adheres the two adherends and topologically entangles with short-chain microgels. In the swollen state, the short-chain microgels restrict the swell of the long-chain polymer network. Ahead of a crack tip, short-chain microgels firstly fracture and the long-chain polymer chains are released to resist load.

2. Experiments

Following [38], we prepare poly (2-acrylamido-2-methyl-1-propanesulfonic acid) (PAMPS) as short-chain microgels and polyacrylamide (PAAm) as long-chain network. To demonstrate the microgel-reinforced hydrogel as an adhesive, we use two pieces of nylon cloth as adherends. We compare two adhesives: PAAm hydrogel adhesives and microgel–PAAm hydrogel adhesives (MPAAm).

2.1. Sample preparation

Most of chemical reagents were purchased from Aladdin, including acrylamide (AAm, monomer), N,N′-methylenebis (acrylamide) (MBAA, crosslinker), ammonium persulfate (APS, initiator), α-ketoglutaric acid (OA, initiator) and N,N,N′,N′-tetramethylethylenediamine (TEMED, accelerator). 2-acrylamido-2-methyl-1-propanesulfonic acid sodium salt solution (AMPS, monomer) was purchased from Sigma-Aldrich. All materials were used as received.

The pure long-chain PAAm adhesive samples were prepared as follows. We first prepared the precursor of long-chain network by dissolving 7 g of AAm, 0.0002 g of MBAA, 0.0025 g of APS, and 7.5 μL of TEMED in 18 g of deionized water. Two pieces of nylon cloth of the size $75\times15\times0.85$ mm^3 were overlapped. The precursor was sprayed in the middle of the two pieces of cloth. The sample was placed between two glass plates covered by polyester films. A silicone rubber frame with the inner size of $75\times15\times1.7$ mm^3 was also placed surrounding the sample between two glass plates to prevent the precursor from flowing away before gelation. Then the sample was cured by an ultraviolet lamp of 15 W and 365 nm at 25 °C for 8h in the environment full of nitrogen gas. The average length, width and thickness of the sample are 75 mm, 15 mm and 1.7 mm. To maintain water content, the as-prepared samples were stored in a sealed polyethylene bag before testing. The chain length of PAAm hydrogel adhesives is estimated by the number of monomers between two crosslinks $n_{PAAm} = \frac{n_{AAm}}{2n_{MBAA}} = 37957$, where n_{AAm} and n_{MBAA} are the moles of AAm and MBAA in the AAm solution.

The PAMPS microgels were prepared as follows. We first prepared an aqueous solution of 1 mol/L AMPS and then added to the solution 4 mol% MBAA and 0.1 mol% OA relative to AMPS. The aqueous solution was injected into a silicone rubber frame with the inner size of $10\times10\times2$ mm^3 and covered with a pair of glass plates. The PAMPS network was cured by the ultraviolet lamp at 25 °C for 8 h in the environment full of nitrogen gas. Then, the PAMPS hydrogel was frozen by liquid nitrogen and immediately dried by a freeze-drying machine (BIOCOOL FD-1A-80) for 24 h to sublimate all the water. Finally, the dry PAMPS polymer was crumbled to small pieces by hand and then ground into fine particles by a planetary grinder (DECO-PBM-V-0.4L) at a rotation rate of 1000 r/min for 12 h. The granularity distribution of dry PAMPS particles was measured by a size analyzer (LS-909, OMEC MOTORS). The grain size ranges from 0.1 μm to 100 μm and particles of the largest proportion (11.08%) has a grain size of 6.8 μm. The as-prepared PAMPS particles were stored in a sealed polyethylene bag to prevent water absorption. The average chain length of PAMPS is estimated by $n_{PAMPS} = \frac{n_{AMPS}}{2n_{MBAA}} = 12.5$.

Microgels were originally used as inelastic dissipaters to enhance toughness of hydrogels [38]. It was reported that, as the amount of microgels increases, the hydrogel-to-polymer mass ratio of swollen microgel-reinforced hydrogels first decreases and then increases [39]. In the present work, the amount of microgels was chosen as follows. We simply adopt the ratio of PAMPS network to PAAm network in double-network hydrogels in our previous paper [19]. We multiply the ratio by the monomer concentration of the AAm precursor and calculate the amount of dry PAMPS particles to be 0.02 g per gram of the AAm solution. For the purpose of restricting swell, the optimal amount of microgels in the present work needs further studies.

The microgel-reinforced hydrogel adhesive samples were prepared as follows. We first prepared the AAm solution as above and added 0.02 g dry PAMPS particles per gram of the AAm solution. The solution with microgels was mixed and placed in a refrigerator at 7 °C for 12 h. After PAMPS microgels swelled to equilibrium, the transparent aqueous AAm solution changed to a homogeneous, viscous, translucent liquid. The as-prepared mixture was sprayed in the middle of the two cloth layers. The size of the pores in the cloth (∼50 μm) was larger than the diameter of the swollen microgels (∼15 μm). The cloth layers were placed for 5 min so that the mixture can penetrate the cloth for a certain depth. The curing procedure is the same as that of PAAm adhesive samples. The as-prepared samples were stored in a sealed polyethylene bag before testing.

To measure the water-to-hydrogel mass ratios of hydrogel adhesives, we prepared bulk hydrogel samples. For PAAm hydrogel samples, we prepared the AAm solution as above. For MPAAm hydrogel samples, we added 0.02 g dry PAMPS particles to each gram of the AAm solution, and mixed and placed the mixture in a refrigerator at 7 °C for 12 h to swell the microgels to equilibrium. The AAm solution and the mixture with microgels were respectively injected into a silicone rubber frame with the inner size of $10\times10\times0.5$ mm^3 and covered with a pair of glass plates. The PAAm hydrogel and MPAAm hydrogel were cured by the ultraviolet lamp at 25 °C for 8 h in the environment full of nitrogen gas. We submerged the as-prepared hydrogel samples in deionized water for 3 days to swell to equilibrium. We cut the hydrogels into 3 pieces with the area of 2×2 mm^2 and measured the mass of each piece, m_{gel}. Then all pieces of hydrogel samples were frozen by liquid nitrogen and dried by the freeze-drying machine for 24 h to sublimate all the water. The mass of dry samples, $m_{polymer}$, was measured. The water-to-hydrogel mass ratio, $W_{water} = \frac{(m_{gel}-m_{polymer})}{m_{gel}}$, is measured to be 68% for both the as-prepared PAAm hydrogels and MPAAm hydrogels, 96% for the swollen PAAm hydrogels, and 88% for the swollen MPAAm hydrogels.

2.2. Fracture and fatigue tests

We submerged the as-prepared adhesive samples in deionized water and recorded the change of mass as a function of time (Fig. 3a). The swelling mass ratio is the mass of the swollen adhesive samples divided by the mass of the as-prepared adhesive samples. The equilibrium swelling mass ratios are 2.81 for the PAAm adhesive sample and 1.75 for the MPAAm adhesive sample. Both samples reached equilibrium after about 1 day.

We adopted the 180-degree peel to measure the adhesion energy and fatigue threshold (Fig. 3b) [25]. The as-prepared adhesive samples were precut using a razor blade in the middle of the two pieces of cloth. The average length of precut is 15 mm. The swollen adhesive samples were prepared by immersing the precut as-prepared adhesive samples in deionized water for 3 days to swell to equilibrium. One leg of cloth separated by the precut was clamped on the fixed lower gripper of the tensile machine (SHIMADZU AGS-X). The other leg of cloth was clamped by the movable upper gripper. We used a load cell of 500 N.

Because the elastic modulus of nylon cloth is on the order of GPa, the cloth-adhesive composite is considered as inextensible. The energy release rate for the 180-degree peel takes the form [40]

$$G = \frac{2F}{w} \tag{1}$$

where F is the force applied by the tensile machine, and w is the width of the adhesive sample.

We first applied a monotonic load at a velocity of 60 mm/min to samples to measure the adhesion energy. The force–displacement curves were recorded by the tensile machine (Fig. 3c). As the applied force increased, the precut crack first opened, blunted but did not extend. When the force reached the plateau, the crack began to propagate and finally reached a steady state. The adhesion energy is obtained as, $\Gamma = 2F_{steady-state}/w$.

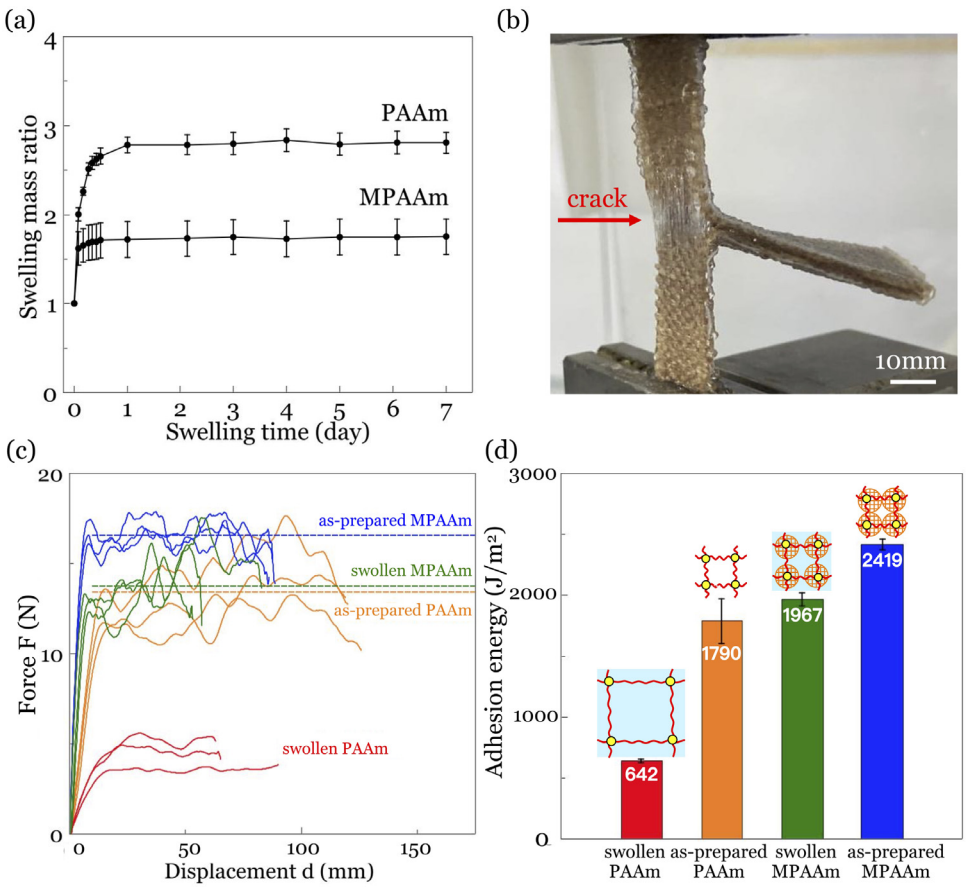

Fig. 3. Swelling and adhesion properties. (a) Swelling mass ratios of adhesive samples as functions of swelling time. (b) The 180-degree peel test of a typical adhesive sample. (c) The force–displacement curves. (d) The adhesion energy.

Each kind of adhesive sample was repeatedly tested for at least three times. The tests were carried out at 25 °C in the open air. The duration of each test was less than 90 s. The water content of each adhesive remained unchanged during the tests.

Next, we applied cyclic loads to study the fatigue of adhesion. Each load cycle ranged from the minimum force $F_{MIN} = 0$ to a given maximum force F_{MAX}. The upper gripper was moved at a constant velocity of 60 mm/min. The force–displacement curves of samples under cyclic loads over cycles were recorded by the tensile machine [25]. Due to the inextensible cloth layers, the difference of displacement at the maximum force between cycles is twice of the crack growth, $\Delta d = 2\Delta c$. The fatigue tests were carried out at 25 °C. To maintain water content, the adhesive samples were sealed in a homemade acrylic chamber and the vapor of deionized water was continuously sprayed on the inner surface of the chamber by a humidifier. The mass of each sample changed less than 9% during the test.

3. Results

The adhesion energy is calculated by substituting the force at the plateau in Fig. 3c to Eq. (1). The average adhesion energies are 642 J/m^2 for swollen PAAm, 1790 J/m^2 for as-prepared PAAm, 1967 J/m^2 for swollen MPAAm, and 2419 J/m^2 for as-prepared MPAAm (Fig. 3d).

Fig. 4a–d shows the crack growth as a function of the number of cycles under cyclic loads of various amplitudes, represented by the energy release rates $G = 2F_{MAX}/w$. In the initial thousands of cycles, the crack growth rate changes, possibly due to the irregular shape of the precut made by the razor blade. After around a 1 mm crack growth, the crack propagates at a constant rate in the steady state. The crack growth per cycle in the steady state is obtained by a linear fit of this region. When the energy release rate is below a threshold, no crack growth can be detected within tens of thousands of cycles. The resolution of crack growth is estimated by the displacement of the gripper of the tensile machine, which is listed as 10 μm by the manufacturer.

Fig. 4e–h plots the crack growth per cycle dc/dN in the steady state as a function of the applied energy release rate G. When the energy release is far above the fatigue threshold, the crack grows fast. When the energy release rate approaches the fatigue threshold, the crack ceases to grow. Compared to the PAAm adhesive samples, the MPAAm adhesive samples have a much smaller crack growth rate under the same G. In experiments, the minimum crack growth measured are on the order of 10^{-8} m/cycle for swollen PAAm, 10^{-9} m/cycle for as-prepared PAAm, 10^{-9} m/cycle for swollen MPAAm and 10^{-10} m/cycle for as-prepared MPAAm.

We adopt the following procedure to estimate the fatigue threshold [41]. We linearly extrapolate the data points in the plane of dc/dN and G (Fig. 4e–h). We use the data close to the G axis and ignore the data far away. The intercept of the G axis gives the experimental fatigue threshold. The fatigue thresholds are 61 J/m^2 for swollen PAAm, 257 J/m^2 for as-prepared PAAm, 262 J/m^2 for swollen MPAAm and 393 J/m^2 for as-prepared MPAAm (Fig. 5).

4. Discussion and conclusion

The adhesion energy of as-prepared MPAAm hydrogel adhesive 2419 J/m^2 is higher than that of as-prepared PAAm hydrogel adhesive 1790 J/m^2. The toughening mechanism of microgels has been explained in Ref [38]. Submerged in water, the adhesion

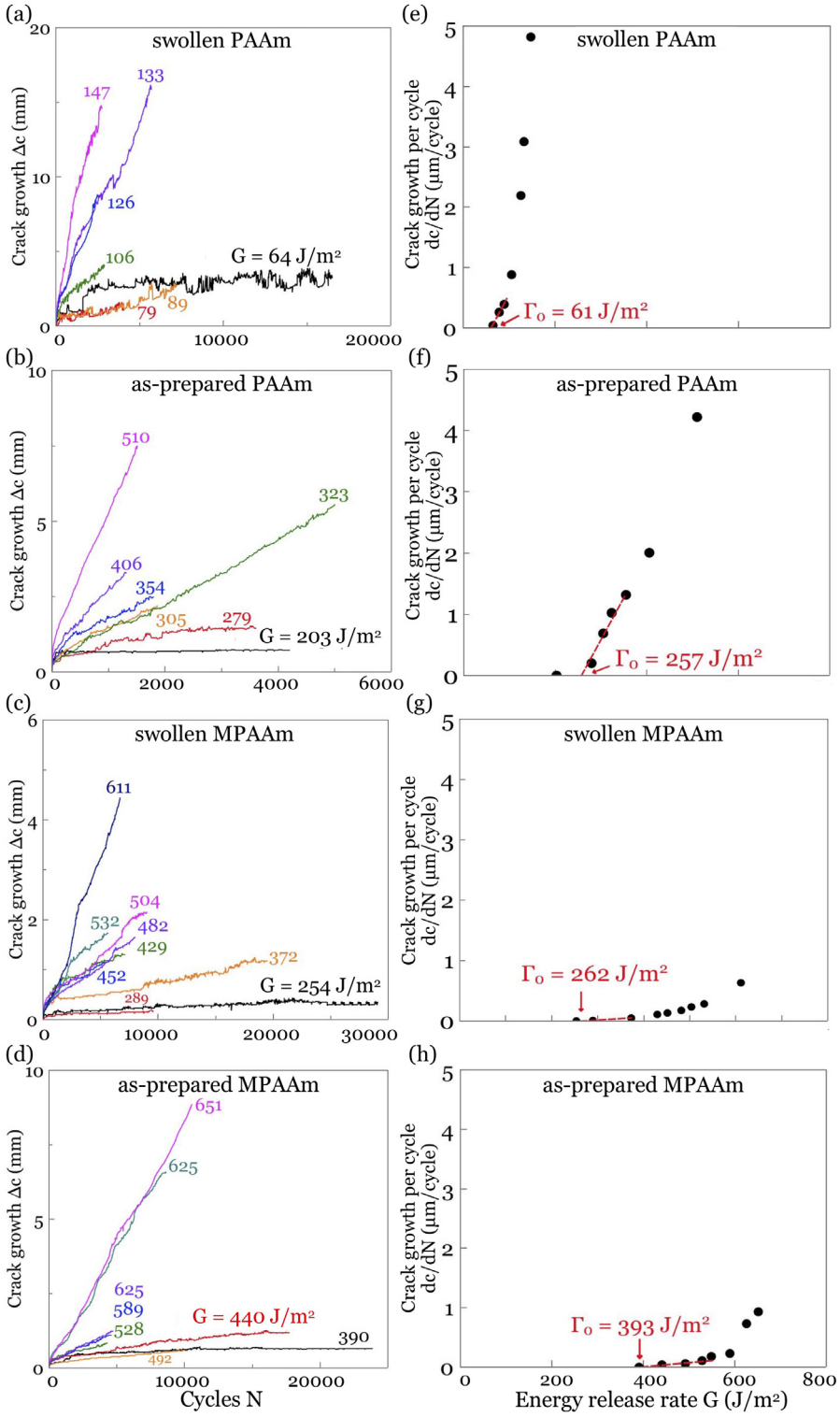

Fig. 4. Fatigue fracture in four kinds of adhesives subject to cyclic load of several amplitudes, as represented by the values of the energy release rate G. (a–d) The crack growth as a function of the number of cycles at several values of G. (e–h) The crack growth per cycle as a function of G. The data points near the G axis are linearly extrapolated to obtain the fatigue threshold.

energy decreased from 1790 J/m^2 for as-prepared PAAm hydrogel adhesive to 642 J/m^2 for swollen PAAm hydrogel adhesive. By adding short-chain microgels, the swollen MPAAm hydrogel adhesive has a high adhesion energy of 1967 J/m^2.

Submerged in water, the adhesive at the crack tip is nearly unconstrained by the adherends and swells freely to equilibrium (Fig. 1b). Assume the as-prepared adhesive layer has a polymer volume fraction of ϕ and the corresponding fatigue threshold is Γ_0. After swelling, the volume fraction of polymer at the crack tip changes to ϕ_s. The linear swelling ratio from the as-prepared state to the swollen state is $\lambda_s = (\phi/\phi_s)^{1/3}$. According to the Lake–Thomas model, the fatigue threshold of polymer network is equal to all the released energy of C–C bonds between two layers of crosslinks as the crack advances per unit area [27]. The model

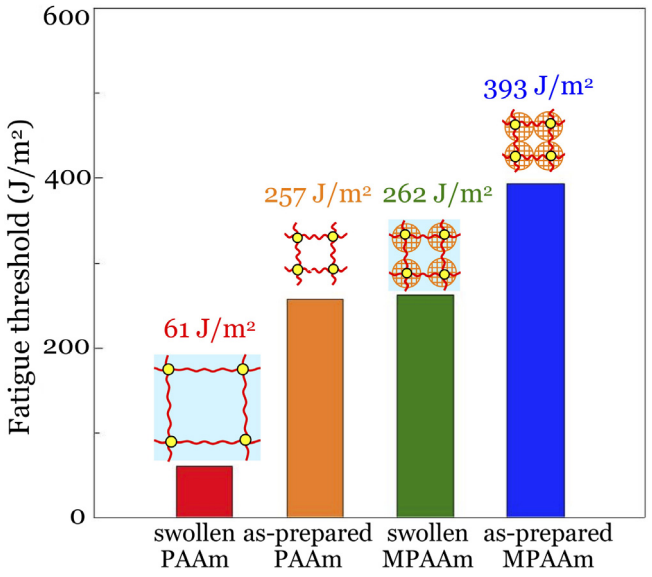

Fig. 5. Fatigue thresholds of the four types of adhesives.

ignores the contribution of entropic elastic energy of polymer chains to the fatigue threshold, because this part is often much less than the internal energy of C–C bonds. Therefore, for the swollen polymer, as the crack advances per unit area the number of encountered polymer chains reduces by λ_s^2, so that the fatigue threshold reduces to $\Gamma_s = \Gamma_0/\lambda_s^2$.

For the PAAm hydrogel, the water-to-hydrogel mass ratio is 68% for the as-prepared hydrogel, and is 96% for the swollen hydrogel, giving the linear swelling ratio $\lambda_s = 2.05$. The fatigue threshold is 257 J/m^2 for the as-prepared hydrogel adhesive. The calculated fatigue threshold in the swollen hydrogel adhesive is $\Gamma_s = \Gamma_0/\lambda_s^2 = 257/2.05^2 = 61$ J/m^2, which happens to be the same as the measured value. For the MPAAm hydrogel, the water-to-hydrogel mass ratio is 68% for the as-prepared gel and is 88% for the swollen gel, giving the linear swelling ratio $\lambda_s = 1.39$. The fatigue threshold of the as-prepared MPAAm adhesive is 393 J/m^2. The calculated fatigue threshold in the swollen state is $393/1.39^2 = 203 J/m^2$, which is somewhat lower than the measured value 262 J/m^2. The fatigue threshold of the as-prepared MPAAm adhesive 393 J/m^2 is higher than that of the as-prepared PAAm adhesive 257 J/m^2. The mechanism of this difference is unclear to us at this writing.

We demonstrate that microgel-reinforced hydrogel adhesive has high fatigue threshold after swell in water to equilibrium. The long-chain network adheres the two adherends, acting as an elastic dissipater to enhance the fatigue threshold. The microgels topologically entangle with the long-chain network, restricting its swell. The microgels also significantly reduce the rate of crack growth under cyclic load above the fatigue threshold.

Declaration of competing interest

The authors declare that they have no known competing financial interests or personal relationships that could have appeared to influence the work reported in this paper.

Acknowledgments

TL acknowledges the support of NSFC, China (11922210, 11772249). JH acknowledges the support of NSFC, China (11702207).

References

[1] I. Skeist, Handbook of Adhesives, Champman & Hall, 1990.
[2] J. Li, A.D. Celiz, J. Yang, Q. Yang, I. Wamala, W. Whyte, B.R. Seo, N.V. Vasilyev, J.J. Vlassak, Z. Suo, D.J. Mooney, Tough adhesives for diverse wet surfaces, Science 357 (6349) (2017) 378–381.
[3] B. Sharma, S. Fermanian, M. Gibson, S. Unterman, D.A. Herzka, B. Cascio, J. Coburn, A.Y. Hui, N. Marcus, G.E. Gold, J.H. Elisseeff, Human cartilage repair with a photoreactive adhesive-hydrogel composite, Sci. Transl. Med. 5 (2013) 167ra6.
[4] N. Lang, M.J. Pereira, Y. Lee, I. Friehs, N.V. Vasilyev, E.N. Feins, K. Ablasser, E.D. O'cearbhaill, C. Xu, A. Fabozzo, R. Padera, S. Wasserman, F. Freudenthal, L.S. Ferreira, R. Langer, J.M. Karp, P.J. del Nido, A blood-resistant surgical glue for minimally invasive repair of vessels and heart defects, Sci. Transl. Med. 6 (2014) 218ra6.
[5] N. Annabi, Y.N. Zhang, A. Assmann, E.S. Sani, G. Cheng, A.D. Lassaletta, A. Vegh, B. Dehghani, G.U. Ruiz-Esparza, X. Wang, S. Gangadharan, A.S. Weiss, A. Khademhosseini, Engineering a highly elastic human protein–based sealant for surgical applications, Sci. Transl. Med. 9 (410) (2017) eaai7466.
[6] J. Li, D.J. Mooney, Designing hydrogels for controlled drug delivery, Nat. Rev. Mater. 1 (12) (2016) 1–17.
[7] T.R. Hoare, D.S. Kohane, Hydrogels in drug delivery: Progress and challenges, Polymer 49 (8) (2008) 1993–2007.
[8] H. Yuk, B. Lu, X. Zhao, Hydrogel bioelectronics, Chem. Soc. Rev. 48 (6) (2019) 1642–1667.
[9] H.R. Lee, C.C. Kim, J.Y. Sun, Stretchable ionics–a promising candidate for upcoming wearable devices, Adv. Mater. 30 (42) (2018) 1704403.
[10] C. Yang, Z. Suo, Hydrogel ionotronics, Nat. Rev. Mater. 3 (6) (2018) 125.
[11] R.J. LaPorte, Hydrophilic Polymer Coatings for Medical Devices, CRC Press, New York, 1997.
[12] H. Cheng, K. Yue, M. Kazemzadeh-Narbat, Y. Liu, A. Khalilpour, B. Li, Y.S. Zhang, N. Annabi, A. Khademhosseini, Mussel-inspired multifunctional hydrogel coating for prevention of infections and enhanced osteogenesis, ACS Appl. Mater. Inter. 9 (2017) 11428.
[13] S. Rose, A. Prevoteau, P. Elzière, D. Hourdet, A. Marcellan, L. Leibler, Nanoparticle solutions as adhesives for gels and biological tissues, Nature 505 (7483) (2014) 382–385.
[14] H. Yuk, C.E. Varela, C.S. Nabzdyk, X. Mao, R.F. Padera, E.T. Roche, X. Zhao, Dry double-sided tape for adhesion of wet tissues and devices, Nature 575 (2019) 169–174.
[15] V. Bhagat, M.L. Becker, Degradable adhesives for surgery and tissue engineering, Biomacromolecules 18 (10) (2017) 3009–3039.
[16] H. Yuk, T. Zhang, S. Lin, G.A. Parada, X. Zhao, Tough bonding of hydrogels to diverse non-porous surfaces, Nature Mater. 15 (2) (2016) 190–196.
[17] J.-Y. Sun, X. Zhao, W.R.K. Illeperuma, O. Chaudhuri, K.H. Oh, D.J. Mooney, J.J. Vlassak, Z. Suo, Highly stretchable and tough hydrogels, Nature 489 (7414) (2012) 133–136.
[18] X. Ni, C. Chen, J. Li, Interfacial fatigue fracture of tissue adhesive hydrogels, Extreme Mech. Lett. 34 (2020) 100601.
[19] W. Zhang, X. Liu, J. Wang, J. Tang, J. Hu, T. Lu, Z. Suo, Fatigue of double-network hydrogels, Eng. Fract. Mech. 187 (2018) 74–93.
[20] Y. Zhou, W. Zhang, J. Hu, J. Tang, C. Jin, Z. Suo, T. Lu, The stiffness-threshold conflict in polymer networks and a resolution, J. Appl. Mech. 87 (3) (2020).
[21] S. Lin, X. Liu, J. Liu, H. Yuk, H. Loh, G.A. Parada, C. Settens, J. Song, A. Masic, G.H. McKinley, X. Zhao, Anti-fatigue-fracture hydrogels, Sci. Adv. 5 (1) (2019) eaau8528.
[22] S. Lin, J. Liu, X. Liu, X. Zhao, Muscle-like fatigue-resistant hydrogels by mechanical training, P. Natl. Acad. Sci. 116 (21) (2019) 10244–10249.
[23] C. Xiang, Z. Wang, C. Yang, X. Yao, Y. Wang, Z. Suo, Stretchable and fatigue-resistant materials, Mater. Today 34 (2019) 7–16.
[24] C. Li, H. Yang, Z. Suo, J. Tang, Fatigue-resistant elastomers, J. Mech. Phys. Solids 134 (2020) 103751.
[25] W. Zhang, Y. Gao, H. Yang, Z. Suo, T. Lu, Fatigue-resistant adhesion I. Long-chain polymers as elastic dissipaters, Extreme Mech. Lett. 39 (2020) 100813.
[26] J. Steck, J. Kim, J. Yang, S. Hassan, Z. Suo, Topological adhesion. I. Rapid and strong topohesives, Extreme Mech. Lett. 39 (2020) 100803.
[27] G.J. Lake, A.G. Thomas, The strength of highly elastic materials, Proc. R. Soc. Lond. Ser. A Math. Phys. Sci. 300 (1460) (1967) 108–119.
[28] E. Zhang, R. Bai, X.P. Morelle, Z. Suo, Fatigue fracture of nearly elastic hydrogels, Soft Matter 14 (2018) 3563–3571.
[29] H. Omidian, S.A. Hashemi, F. Askari, S. Nafisi, Swelling and crosslink density measurements for hydrogels, Iranian J. Polym. Sci. Tech. 3 (2) (1994).
[30] B. Liu, Y. Wang, Y. Miao, X. Zhang, Z. Fan, G. Singh, X, Zhang, K. Xu, B. Li, Z. Hu, M. Xing, Hydrogen bonds autonomously powered gelatin methacrylate hydrogels with super-elasticity, self-heal and underwater self-adhesion for sutureless skin and stomach surgery and E-skin, Biomaterials 171 (2018) 83–96.

[31] J.Y. Kim, S.B. Ryu, K.D. Park, Preparation and characterization of dual-crosslinked gelatin hydrogel via Dopa-Fe^{3+} complexation and fenton reaction, J. Ind. Eng. Chem. 58 (2018) 105–112.
[32] K. Haraguchi, T. Takehisa, Nanocomposite hydrogels: A unique organic–inorganic network structure with extraordinary mechanical, optical, and swelling/de-swelling properties, Adv. Mater. 14 (16) (2002) 1120–1124.
[33] P. Schexnailder, G. Schmidt, Nanocomposite polymer hydrogels, Colloid Polym. Sci. 287 (2009) 1–11.
[34] S. Abdurrahmanoglu, V. Can, O. Okay, Design of high-toughness polyacrylamide hydrogels by hydrophobic modification, Polymer 50 (2009) 5449–5455.
[35] H. Kamata, Y. Akagi, Y. Kayasuga-Kariya, U. Chung, T. Sakai, Nonswellable hydrogel without mechanical hysteresis, Science 343 (6173) (2014) 873–875.
[36] A. Agrawal, N. Rahbar, P.D. Calvert, Strong fiber-reinforced hydrogel, Acta Biomater. 9 (2013) 5313–5318.
[37] J.P. Gong, Y. Katsuyama, T. Kurokawa, Y. Osada, Double-network hydrogels with extremely high mechanical strength, Adv. Mater. 15 (14) (2003) 1155–1158.
[38] J. Hu, K. Hiwatashi, T. Kurokawa, S.M. Liang, Z.L. Wu, J.P. Gong, Microgel-reinforced hydrogel films with high mechanical strength and their visible mesoscale fracture structure, Macromolecules 44 (19) (2011) 7775–7781.
[39] J. Hu, T. Kurokawa, K. Hiwatashi, T. Nakajima, Z.L. Wu, S.M. Liang, J.P. Gong, Structure optimization and mechanical model for microgel-reinforced hydrogels with high strength and toughness, Macromolecules 45 (12) (2012) 5218–5228.
[40] R.S. Rivlin, A.G. Thomas, Rupture of rubber. I. Characteristic energy for tearing, J. Polym. Sci. 10 (3) (1953) 291–318.
[41] R. Bai, Q. Yang, J. Tang, X.P. Morelle, J. Vlassak, Z. Suo, Fatigue fracture of tough hydrogels, Extreme Mech. Lett. 15 (2017) 91–96.